KERNFORSCHUNGSZENTRUM

KARLSRUHE

Mai 1973 KFK 1730

Institut für Radiochemie

A Comparison of Models for Calculating Excitation Functions

H.F. Röhm, K.A. Keller, H. Münzel

GESELLSCHAFT
FÜR
KERNFORSCHUNG M.B.H.

KARLSRUHE

GESELLSCHAFT FÜR KERNFORSCHUNG M. B. H.
KARLSRUHE

KERNFORSCHUNGSZENTRUM KARLSRUHE

KFK 1730

Institut für Radiochemie

A Comparison of Models for Calculating Excitation Functions

by

H.F. Röhm, K.A. Keller and H. Münzel

Gesellschaft für Kernforschung m.b.H., Karlsruhe

Abstract

The comparison of models for calculating excitation functions was based on the deviations between calculated and measured excitation functions for about 180 different reactions, induced by neutrons, protons, ^{3}He and α-particles, with target nuclei having proton numbers ranging from 13 to 92. In addition, input parameters and their influence on the form of excitation functions are discussed.

Zusammenfassung

Gestützt auf die Abweichungen zwischen berechneten und experimentellen Anregungsfunktionen werden theoretische Ansätze zur Berechnung von Anregungsfunktionen verglichen. Die Bewertung erfolgt auf der Grundlage von 180 experimentell bestimmten Anregungsfunktionen von Kernreaktionen mit n,p,^{3}He und α als Projektil auf Targetkerne mit Protonenzahlen zwischen 13 und 92. Außerdem werden Modellparameter und ihr Einfluß auf die Form der Anregungsfunktion diskutiert.

Contents

1. Introduction

The calculation of excitation functions at low and medium energies has become well established over the years and has withstood the test of comparison with experiment. In fact, the reported agreement between measured and calculated excitation functions seems to be so satisfactory that a number of differing calculations for computing excitation functions have established themselves. The various types of calculations usually differ in their complexity, i.e. the computations differ in the degree of approximations introduced, and in the methods applied for numerical evaluation of the appropriate equations. It should be stated that controversy persists about the validity and region of applicability of the simplifications introduced in the various calculations.

To our knowledge, it has yet to be reported which type of calculation and what values for the input parameters would give the best results for many reaction types over a wide range of projectiles and target nuclei. This is the purpose of the present work.

The appraisal of merit is based on deviations between calculated and measured excitation functions, which includes all attempts to obtain "best-fits" by adjusting the input parameters. A sample size of 30 articles published from 1959 to 1972 has been used for this purpose. In each of these articles, the authors have calculated excitation functions and compared them to their own experimental measurements or have taken another's experimental values. Figure 1 shows the range of different target nuclei and projectiles producing nuclear reactions leading to the excitation functions, calculated and measured, contained in the 30 articles. This amounts to about 180 measured excitation functions for different reactions of the type (——,xn yp zα), where $0 \leq x \leq 8$, $0 \leq y \leq 3$ and $0 \leq z \leq 2$. The range of the proton numbers of the target nuclei for these reactions is between 13 and 92. The projectiles inducing these reactions are neutrons, protons, ^{3}He and α-particles with kinetic energies up to 120 MeV.

Zum Druck eingereicht am 17.4.1973

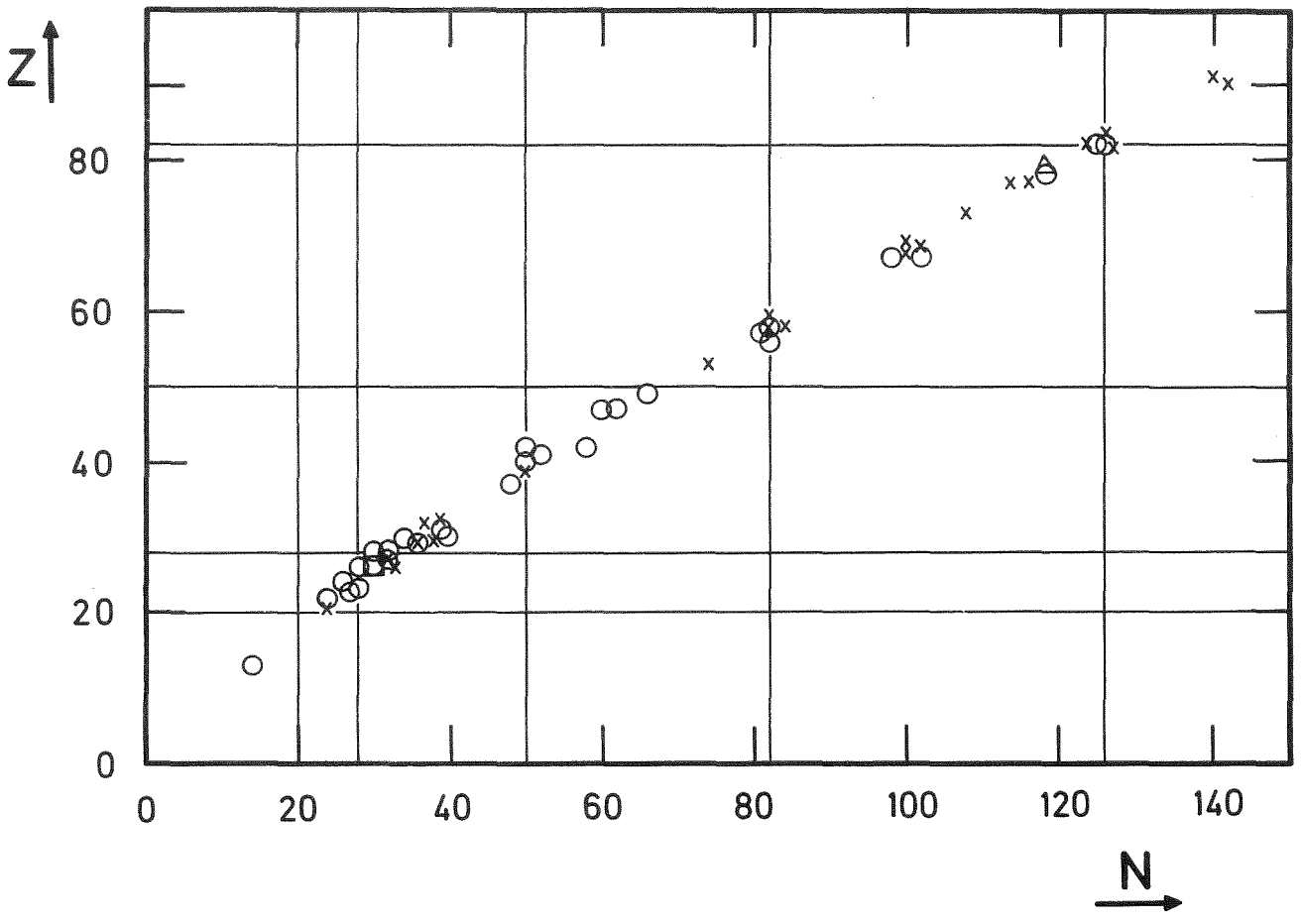

Figure 1. The target nuclei of different reactions for the excitation functions, contained in the 30 articles used in this survey, are shown. The ordinate is the proton number (atomic number) Z and the abscissa the neutron number N. The solid lines show the neutron and proton magic numbers and the symbols used to characterize the projectiles inducing the reactions are:

□ n X p

△ ^{3}He O α

2. Classification of Computational Categories for the Calculation of Excitation Functions

In order to establish which models and different modes of calculation give the best agreement with experiment, the various methods of calculating excitation functions were roughly categorized into different classes as described below. Since the input parameters often influence each other and depend much on the form of the equation in which they are contained, this classification also facilitates a means with which the reported values of parameters that belong to one class may be directly compared.

The equations of the different models can either be evaluated analytically or by Monte Carlo technique. Both modes should give identical results. This distinction was introduced in order to see whether any differences could possibly be seen when compared with one another.

Table I. Computational categories for calculating excitation functions

Model	Mode of calculation	Class K
Compound-equilibrium including angular momentum	Analytic	1
	Monte Carlo	2
Compound-equilibrium without angular momentum	Analytic	3
	Monte Carlo	4
Intra-nuclear-cascade-evaporation	Analytic*	5
	Monte Carlo*	6
Compound-pre-equilibrium	Analytic	7

*Analytic and Monte Carlo refer here only to the evaporation step of the calculation.

For all classes, only those parameters and formulae pertaining to the statistical model are discussed. For instance, parameters due to the optical model were disregarded.

3. Criteria for the Comparison between Calculated and Measured Excitation Functions

In this section, the basis is outlined on which the appraisal of merit rests for the various classes K (i.e. the different methods of calculating excitation functions). For this purpose one requires certain magnitudes which are able to characterize several aspects of the form of an excitation function. These were chosen as follows:

M, the maximum cross-section value,
P, the position of M on the energy axis,
FW, the full-width at one half M,
SL, the low-energy flank's slope at one half M and
SH, the high-energy flank's slope at one half M.

These magnitudes were extracted from all the calculated and corresponding experimentally determined excitation functions contained in the 30 articles and the relative percentage errors were calculated as shown in equations 1a to 1e. The subscripts are self-explanatory.

Maximum cross section: $$\left(\frac{\Delta M}{M}\right) = \frac{M_{cal} - M_{exp}}{M_{exp}} 100 \qquad (1a)$$

Position: $$\left(\frac{\Delta P}{P}\right) = \frac{P_{cal} - P_{exp}}{10} 100 \qquad (1b)$$

Full-width: $$\left(\frac{\Delta FW}{FW}\right) = \frac{FW_{cal} - FW_{exp}}{FW_{exp}} 100 \qquad (1c)$$

Low-energy slope: $$\left(\frac{\Delta SL}{SL}\right) = \frac{SL_{exp} - SL_{cal}}{SL_{exp}} 100 \qquad (1d)$$

High-energy slope: $$\left(\frac{\Delta SH}{SH}\right) = \frac{SH_{exp} - SH_{cal}}{SH_{exp}} 100 \qquad (1e)$$

The sign of the equations 1a to 1c were chosen such that the relative percentage errors are negative if the calculated values are smaller than the experimental values. In keeping with this, the indexes of equations 1d and 1e were reversed because if the relative percentage errors are negative for

instance this would imply that the calculated cross sections decrease more rapidly than the experimental ones as a function of the projectile energy. This in turn means that the cross sections are underestimated.

The denominator of equation 1b was set equal to an arbitrary value of 10 MeV so that the relative percentage error ($\Delta P/P$) does not depend on the magnitude of P_{exp} for a particular value of the difference ($P_{cal} - P_{exp}$).

For a single article of the class K, the arithmetic means and the corresponding standard deviations were calculated according to equations 2a to 2e and 3a to 3e respectively, where n is the number of the relative percentage errors.

The arithmetic means for the maximum cross section,

$$\overline{\left(\frac{\Delta M}{M}\right)} = \frac{\sum\left(\frac{\Delta M}{M}\right)}{n} \qquad (2a)$$

. . (2b)

. . (2c)

. . (2d)

high-energy slope,

$$\overline{\left(\frac{\Delta SH}{SH}\right)} = \frac{\sum\left(\frac{\Delta SH}{SH}\right)}{n} \qquad (2e)$$

The corresponding standard deviations for the

maximum cross section,

$$\Omega\overline{\left(\frac{\Delta M}{M}\right)} = \sqrt{\frac{\sum\left(\overline{\left(\frac{\Delta M}{M}\right)} - \left(\frac{\Delta M}{M}\right)\right)^2}{n-1}} \qquad (3a)$$

. . (3b)

. . (3c)

. . (3d)

high-energy slope,

$$\Omega\overline{\left(\frac{\Delta SH}{SH}\right)} = \sqrt{\frac{\sum\left(\overline{\left(\frac{\Delta SH}{SH}\right)} - \left(\frac{\Delta SH}{SH}\right)\right)^2}{n-1}} \qquad (3e)$$

For a single publication and class K, a total error - MEAN $\pm$ SD - was determined from the individual errors and is given by,

$$\text{MEAN} \pm \text{SD} = \frac{\left|\left(\overline{\frac{\Delta M}{M}}\right)\right| + \left|\left(\overline{\frac{\Delta P}{P}}\right)\right| + \left|\left(\overline{\frac{\Delta FW}{FW}}\right)\right| + \left|\left(\overline{\frac{\Delta SL}{SL}}\right)\right| + \left|\left(\overline{\frac{\Delta SH}{SH}}\right)\right|}{5} \tag{4}$$

$$\pm \quad \frac{\left|\Omega\left(\overline{\frac{\Delta M}{M}}\right)\right| + \left|\Omega\left(\overline{\frac{\Delta P}{P}}\right)\right| + \left|\Omega\left(\overline{\frac{\Delta FW}{FW}}\right)\right| + \left|\Omega\left(\overline{\frac{\Delta SL}{SL}}\right)\right| + \left|\Omega\left(\overline{\frac{\Delta SH}{SH}}\right)\right|}{5}$$

The values MEAN $\pm$ SD, expressed as percentages, formed the basis for intercomparison of methods for calculating excitation functions.

4. The Class K = 1,2 Calculations

4.1. Deviations of the Calculated Excitation Functions

For the comparison of classes K = 1,2, 10 publications were considered in which calculations were performed for various reactions on target nuclei varying in proton number from Z = 13 to Z = 79. The number of measured excitation functions used in these publications for comparison with the computed results range from two to twelve per publication. On the average, only 5 experimentally measured excitation functions (and usually only for one element) are used in a single article, which then forms the basis for substantiating the degree of success of the calculations performed. These, in our opinion, are too few experimental data to justify far reaching conclusions about the applied method of calculation in one article alone.

The deviations of the calculated excitation functions from the corresponding experimental values, per class K and article, are plotted in figure 2 for each of the characteristic magnitudes M, P, FW, SL, and SH. The values for $\overline{(\Delta M/M)}$, $\overline{(\Delta P/P)}$, $\overline{(\Delta FW/FW)}$, $\overline{(\Delta SL/SL)}$ and $\overline{(\Delta SH/SH)}$ are plotted in this order and are distinguished by different symbols. These values are joined by straight lines for each article. The error bars correspond to $\pm\ \Omega\overline{(\Delta M/M)}$, $\pm\ \Omega\overline{(\Delta P/P)}$, ... etc. The articles are arranged from left to right in increasing order of the proton number of the target nucleus. Furthermore, at the top of the figure are listed per article: the class K, the article number (references of which are to be found in Appendix A), the number of experimental excitation functions used for comparison, the Z-range of the target nuclei and finally the projectile energy range (in MeV) over which the experimental data and calculations extend. The MEAN $\pm$ SD values for each article are tabulated at the bottom of the figure. It must be stressed that only those calculated and measured excitation functions, which at least possessed the maximum cross-section values M_{cal} and M_{exp}, were used to calculate the deviations listed above.

It is clear from figure 2 that a relationship exists between the errors $\overline{(\Delta M/M)}$, ..., $\overline{(\Delta SH/SH)}$ for each publication, regardless of whether K = 1 or K = 2. For instance, if $\overline{(\Delta M/M)} > 0$, i.e. $M_{cal} > M_{exp}$, then both $\overline{(\Delta SL/SL)} < 0$ and $\overline{(\Delta SH/SH)} < 0$, i.e. $SL_{cal} > SL_{exp}$ and $SH_{cal} > SH_{exp}$. This means that if the calculated

maximum cross section is overestimated, then both the low-energy and high-energy flanks of the calculated excitation function will usually have steeper slopes than the corresponding experimental values. The converse is also true, namely if $M_{cal} < M_{exp}$ then the low-energy and high-energy slopes of the calculated excitation functions will generally be less steep than the experimentally measured excitation function. However, for $M_{cal} \gtrless M_{exp}$ the values of both $\overline{(\Delta P/P)}$ and $\overline{(\Delta FW/FW)}$ are less than about $\pm$ 20 %. This means that a calculated over- or under-estimation of the maximum cross-section value has little effect on either its position or the full-width at half-maximum height of the excitation function: it is at least small compared to its effect on the high-energy and low-energy slopes.

If the deviation in the calculated maximum cross section, $(\Delta M/M)$, is large and positive, then it is possible with the aid of publications 19, 30 and 9 to correlate the deviations given by equations 2b to 2e to $(\Delta M/M)$. A first approximation yields $(\Delta P/P) \cong - 0.4\ (\Delta M/M)$, $(\Delta FW/FW) \cong - 0.1\ (\Delta M/M)$, $(\Delta SL/SL) \cong - 0.9\ (\Delta M/M)$ and $(\Delta SH/SH) \cong - (\Delta M/M) - 35$ %.

That the calculated high-energy slope of the excitation function is steeper than the experimental value is not surprising, eventhough on an average good agreement exists for the maximum cross section M, its position P, the full-width at half-maximum height FW and the low-energy slope SL. This is simply due to the fact that the contribution from direct reactions, which are not taken into account in the classes K = 1,2 calculations, becomes increasingly dominant as the excitation energy increases, which thus tends to decrease the slope of the flank of the experimental excitation function on the high-energy side.

Using the results of the publications 7, 14 and 1, with $\Delta M/M \sim 0$, it was possible to roughly estimate the mean of the sum of the $\overline{(\Delta SH/SH)}$-values which was found to be about -35 %. Therefore calculations of the classes K = 1,2 cannot be expected to give a much smaller error than this for the slope on the high-energy flank.

In order to see whether there are in fact any differences between the class K = 1 and K = 2 calculations, the MEAN values were averaged for all the articles belonging to K = 1 and K = 2, separately. The same was carried out for the SD values. This

resulted in 22 $\pm$ 40 % and 18 $\pm$ 34 % for the classes K = 1 and K = 2 respectively. Comparison of these figures indicates no bias for the Monte Carlo calculations. Therefore, all results for both classes were pooled and the overall error thus obtained is 20 $\pm$ 37 %. This means that a calculated excitation function can be expected to deviate from the experimental excitation function for the individual magnitudes M, P, FW, SL and SH by as much as -60 % to +60 %, taking a one sigma confidence limit.

4.2. Parameters used

Because influences due to the optical model calculations have been omitted, the main part in the emission probability for particles is the density ρ of levels having a given spin J. The following equations are used in the publications of classes K = 1,2:

$$\rho(U,J) \propto a^{1/2}\ \theta^{-3/2}(2J+1)U^{-2}\ \exp\left[(4a\ U)^{1/2}\right] \tag{5}$$

$$\rho(U,J) \propto a^{1/2}\ \theta^{-3/2}(2J+1)U^{-2}\ \exp\left[(4aU)^{1/2}\right]\ \exp\left[-\frac{E_{rot}}{t}\right] \tag{6}$$

$$\rho(U,J) \propto a^{1/2}\ \theta^{-3/2}(2J+1)U^{-5/4}\exp\left[(4aU)^{1/2}\right]\exp\left[-\frac{\hbar^2(J+1/2)^2}{2\ \theta\ T}\right] \tag{7}$$

where

- a = level density parameter
- θ = moment of inertia
- J = spin
- U = excitation energy
- E_{rot} = rotational energy
- t = thermodynamic temperature
- T = nuclear temperature

and in Table II

- δ = pairing energy
- ΔE = shell correction energy
- r_o = radius parameter

The controversial parameters in the level density are a, θ, δ and r_o, which enters into a and θ.
Further, in article 14 the Jackson model [1] is used for the evaporation part (see 6.2.).

4.2.1. The Level Density Parameter

This parameter, as derived from the Fermi-gas model is given by

$$a = \frac{A}{C} \qquad (8)$$

where A is the nucleon number and C a constant, into which r_o enters.

Values of C used in the publications are listed in Table II (the target nuclei cover a Z-range between 13 and 79). One would expect C to be more or less constant. However, as is evident from Table II, the values actually applied are 6.0 MeV $\leq$ C $\leq$ 22.0 MeV, i.e. they vary by more than a factor of three. There are two reasons: First, many C-values were not calculated but adjusted in order to facilitate good agreement between experiment and calculations. Second, the value of a is influenced by the choice of other parameters such as θ (cf. article 30) and the γ-ray emission strength constant (cf. article 9). Thus uncertainty exists as to what value of the level density parameter a one should use.

4.2.2. The Moment of Inertia

The moment of inertia appears in the level density formula and is further incorporated in the rotational energy E_{rot}. The value of θ is usually quoted relative to the rigid body value θ_{rig} which is, for a nucleus of spherical shape,

$$\theta_{rig} = \frac{2}{5} r_o^2 A^{5/3} m_N, \qquad (9)$$

where m_N is the mass of the nucleon, and A the nucleon number.

The effect different values of θ have on the form of an excitation function may be summarized as follows (cf. article 3 for example). The value of θ/θ_{rig} was increased from 0.5 to 1.0 in the calculation of the $^{92}Mo(\alpha,n)^{95}Ru$ excitation function and the effect was to lower the maximum cross section M_{cal} somewhat and to shift its position P_{cal} towards lower energies. Although the low-energy slope SL_{cal} was virtually unaltered, considerable changes occured for the full-width FW_{cal} and the high-energy slope SH_{cal}. It was found that the full-width at half-maximum height decreased, while the slope of the high-energy flank increased

Table II: Values used in the different level density formulae for the classes K = 1,2; the articles are arranged in increasing order of the Z-range of the target nuclei

Article No. (Class K)	Corrections for the excitation energy U			C [MeV] in eq. 8	Moment of inertia		γ-ray emission strength constant [erg^{-4} s^{-1}]
	Eq.	Pre-exponential Term	Exponential Term		θ/θ_{rig}	r_o [fm] in eq. 9	
19 (1)	5	δ, E_{rot}	δ, E_{rot}	8.0	1.0		-
8 (2)	5	t, δ, E_{rot}	δ, E_{rot}	12.3	1.0	1.22	$2 \cdot 10^{-5}$
2 (1)	6	t, δ	δ	8.0	0-1.0	-	-
3 (1)	5	δ, E_{rot}	δ, E_{rot}	6.0-10.0	0.35-1.2	-	-
30 (1)		none	none				
		δ	δ				
	5,6	δ, ΔE	δ, ΔE				
		δ, E_{rot}, ΔE	δ, E_{rot}, ΔE	8.0-22.0	0.65-0.9	-	-
		δ, E_{rot}	δ, E_{rot}				
7 (1)	7	T, δ	δ	10.0	1.0	-	-
9 (2)	5	t, δ, E_{rot}	δ, E_{rot}	6.7-15.0	0.5 -1.0	-	$2 \cdot 10^{-5}$-$5 \cdot 10^{-7}$
14 (1)	Jackson model (T=1.66 MeV, see 6.2)				-	-	-
1 (2)	5	t, δ, E_{rot}	δ, E_{rot}	7.5	0-1.0	1.25	$3 \cdot 10^{15}$ *
16 (1)	5	δ, E_{rot}	δ, E_{rot}	8.4	1.0	1.2	-

* The articles 8, 9 and 1 all use the same formalism for the gamma-ray emission strength constant. However, the value given for article 1 differs from the remaining values by factor which is not given explicitly.

considerably. It should be emphasized that all other parameters were kept constant for these calculations. The authors went further and tried to systematize the variation of θ/θ_{rig}, used in their calculations, as a function of the mass number of the product nucleus which varied from 80 to 170. It was found that from nucleon number about 100 onwards, the values of θ/θ_{rig} varied in the narrow range from 0.3 to 0.4, while below nucleon number 100 the value increased to about 1.2.

No such trend in θ/θ_{rig} can be seen in the other publications. Furthermore, according to the systematics of Lange and Münzel [2], the full-width FW of (α,xn) excitation functions decreases with increasing proton number of the target nucleus for most of the reactions. This implies, according to the above-mentioned influence of θ on the form of the excitation function, that θ/θ_{rig} should get larger with increasing nucleon number.

In many publications θ is varied with the excitation energy. This seems to be the best way to incorporate θ in the calculations for the classes K = 1,2.

4.2.3. The Gamma-ray Emission Strength Constant

Another parameter is the gamma-ray emission strength constant C_1, which is listed in table II. This constant may be calculated from theory, but the value actually used in calculations of excitation functions is largely dependent on what the choice of the level density parameter a is, or vice versa.

There is evidently no doubt about the fact that the inclusion of gamma-ray emission leads to the broadening of the excitation function. Therefore a decrease in C_1 (i.e. a decrease of gamma-ray competition with particle emission) leads to a narrowing of the calculated excitation function and a shift in the position of the calculated maximum cross section to lower energies. However, it should also be borne in mind that this variation may also be achieved by changing the value of the moment of inertia, or the level density parameter, which is discussed in section 5.2.1.

4.2.4. The Excitation Energy

In most cases the excitation energy U in the equations 5, 6, 7 is corrected for the pairing effect by means of the term δ. The pairing energy can have a marked effect on the maximum cross section (cf. article 1). This will be discussed in the next class of calculations (see 5.2.2). Furthermore, the rotational energy E_{rot} and a shell correction energy ΔE is introduced. In some cases the thermodynamic temperature t or the nuclear temperature T is added to the excitation energy U in the pre-exponential term. The effect dropping the temperature has is uncertain.

5. The Class K = 3,4 Calculations

The main differences between these methods of calculation and those used for the classes K = 1,2 are that angular momentum effects and gamma-ray emission are disregarded. Therefore it would be expected that the K = 3,4 calculations should give narrower excitation functions with a steeper slope on the high-energy flank. Furthermore, the formation cross section is not always obtained from the optical model, but is often replaced by the geometric cross section which includes a term to account for the Coulomb barrier height.

5.1. Deviations of the Calculated Excitation Functions

The following discussion is based on a sample size of 13 articles, which cover a Z-range from 13 to 82 for the target nuclei. The number of excitation functions, possessing at least a maximum cross-section value, used in each of these articles, vary from 2 to 40. On the average, this means that 5 experimental excitation functions per article form the basis for assessing the "goodness-of-fit" obtained for these calculations. This is comparable to the classes K = 1,2 calculations. Article 12 is not contained in this average since it is an exception that such a large sample of 40 experimental excitation functions has been used in one article alone.

Figure 3 shows a plot of the deviations $\overline{(\Delta M/M)}$, $\overline{(\Delta P/P)}$,.... ect., for each of the articles together with the corresponding error bars $\pm\ \Omega\overline{(\Delta M/M)}$,$\pm\ \Omega\overline{(\Delta P/P)}$,... etc., as in figure 2. It is evident that the trends of the deviations shown in figure 3 are similar to those obtained for the class K = 1,2 calculations (see figure 2). Again, as $\overline{(\Delta M/M)}$ becomes large and positive, so the calculated excitation functions tend to become narrower and the high-energy steeper, i.e. $\overline{(\Delta SH/SH)}$ more negative.

From figure 3, it may be seen that the calculated excitation functions of articles 5, 29, 25 and 26 have smaller deviations for the maximum cross section M, its position P and the full-width FW, than the remaining articles of the class K = 3,4 calculations. Because these errors are small, the values of $\overline{(\Delta SH/SH)}$ will not be

unduly distorted. Consequently these articles can be used to obtain an idea of how much the high-energy slope is underestimated on the average. The arithmetic mean for $\overline{(\Delta SH/SH)}$ for these four articles is -30 %. It is surprising that this percentage is so similar, to -35 % obtained for the classes K = 1,2, because exclusion of angular momentum effects and gamma-ray emission should lead to narrower excitation functions with steeper high-energy slope.

A decrease in the level density parameter a leads to larger full width and larger values for the high energy slope. Thus the effect of excluding angular momentum and γ-ray emission can be compensated for by using small values of a. Therefore in the classes K = 3,4 in general quite smaller values of a were used (see corresponding C-values in Table II and III). Taking a-values similar to the level density parameters in the classes K = 1,2 the deviations in the high energy slope are very large (see fig. 3, articles 18 and 19).

In order to compare the class K = 3 and K = 4, the average of the MEAN $\pm$ SD were determined. The values obtained were 79 $\pm$ 77 % and 44 $\pm$ 76 % for K = 3 and K = 4 respectively. This difference is mainly due to the large deviations in the high-energy slope of the above mentioned articles 18 and 19. Disregarding these two publications the mean value for K = 3 is 31 $\pm$ 43 %.

An attempt was made to see whether any correlation could be found for the deviations $(\Delta P/P)$, $(\Delta FW/FW)$, $(\Delta SL/SL)$ and $(\Delta SH/SH)$ in terms of $(\Delta M/M)$. The following rough estimates were obtained for all articles except 5, 29, 25 and 26:
$(\Delta P/P) \cong -0.1(\Delta M/M)$, $(\Delta FW/FW) \cong -0.3(\Delta M/M)$, $(\Delta SL/SL) \cong -1.2(\Delta M/M)$ and $(\Delta SH/SH) \cong -2.2(\Delta M/M)$ -30 %.

5.2. Parameters used

The The following equations for the level density ρ are used:

$$\rho(U) \propto U^{-2} \exp\left[(4aU)^{1/2}\right] \qquad (10)$$

$$\rho(U) \propto U^{-5/4} \exp\left[(4aU)^{1/2}\right] \qquad (11)$$

$$\rho(U) \propto \exp\left[(4aU)^{1/2}\right] \qquad (12)$$

For explanations see 4.2.

Table III: Values used in the different level density formulae for the classes K = 3,4; the articles are arranged in increasing order of the Z-range of the target nuclei

Article No. (Class K)	Corrections for the excitation energy U			C [MeV] in eq. 8
	Eq.	Pre-exponential Term	Exponential Term	
19 (3)	10	δ	δ	8.0
		δ, ΔE	δ, ΔE	8.0
6 (4)	12	-	δ	20.0
12 (4)	12	-	δ	20.0
13 (4)	12	-	δ	20.0
11 (4)	12	-	δ	20.0
18 (3)	10	δ	δ	8.5
		δ, ΔE	δ, ΔE	8.5
4 (3)	12	-	δ	37.0
5 (3)	12	-	δ	38.0
	10		δ	19.0
29 (3)	12	-	δ	18.0-72.0
27 (3)	12	-	δ	18.0-71.0
16 (3)	10	δ	δ	8.4-25.0
25 (3)	11	δ	δ	11.0
26 (4)	12	-	δ	20.0

5.2.1. The Level Density Parameter

Table III shows that the values of C are exceptionally large compared to those used for the class K = 1,2 calculations and the spread of these values is very large, ranging from 8 MeV to 72 MeV. The values center about C $\approx$ 20 MeV, i.e. a factor of two larger than in the K = 1,2 calculations.

As an example, the influence due to changing the a-values on the deviations (ΔM/M),(ΔP/P),... etc., as well as the mean of these errors, for ^{197}Au(α,xn)-reactions are shown in Table IV. The average of the mean errors in column 8 of Table IV for all the listed reactions are 29 %, 34 % and 59 % for a = 8, 16 and 24 MeV^{-1} respectively. Thus the best overall fit can be obtained with a = 8 MeV^{-1} or even a = 16 MeV^{-1}.

The value for the level density parameter chosen to achieve a "best-fit" value to the experimental excitation function data depends on which form of the level density formula is used. For example, Fukushima et al. [3] used two forms of the level density as depicted by equations 10 and 12 in their calculations of excitation functions. If the level density parameter used in equations 12 and 10 are denoted by a_1 and a_2 respectively, then they found that equally good fits to the experimental results can be obtained with both forms of the level density formula if $a_2 = a_1 + 3.0$ MeV^{-1}.

5.2.2. The Pairing Energy

The pairing energy δ is applied as an energy correction in the level density formula to account for odd-even nuclear effects. There are several ways in which one can arrive at δ-values. The most commonly used are those of Cameron [4].

Dostrovsky at al. [5], investigated the influence the pairing energy term has on the height and the form of excitation functions. They concluded that the relative yields of different evaporated particles are very sensitive to the pairing energy term, whereas the competition between reactions leading to the emission of various numbers of the same particle is more sensitive to the level density parameter a. They also found that δ is not very sensitive to the choice of a.

Table IV: The effect of the level density parameter a on the form of excitation functions for $^{197}Au(\alpha,xn)$ reactions taken from article 16.

Reaction	a [MeV^{-1}]	(ΔM/M) [%]	(ΔP/P) [%]	(ΔFW/FW) [%]	(ΔSL/SL) [%]	(ΔSH/SH) [%]	Mean Error + [%]
(α,2n)	8	53	13	- 1	- 47	- 91	41
(α,2n)	16	47	0	- 23	- 75	- 145	58
(α,2n)	24	43	0	- 33	- 70	- 221	73
(α,3n)	8	24	22	11	- 20	- 24	20
(α,3n)	16	24	0	- 12	- 24	- 69	26
(α,3n)	24	24	0	- 22	- 24	- 137	41
(α,4n)	8	- 9	39	22	28	21	24
(α,4n)	16	4	0	0	- 4	- 16	5
(α,4n)	24	5	- 24	- 11	- 26	- 37	21
(α,5n)	8	34	54	32	- 11	- 28	32
(α,5n)	16	85	0	0	- 94	- 49	46
(α,5n)	24	102	- 20	- 32	-151	- 217	104

$$^{+}\ \text{Mean Error} = \frac{|(\Delta M/M)|+|(\Delta P/P)|+|(\Delta FW/FW)|+|(\Delta SL/SL)|+|(\Delta SH/SH)|}{5}$$

During the course of their investigations, they found that Cameron's pairing values did not lead to satisfactory agreement between calculated and experimental excitation functions. Therefore they developed a procedure for systematizing δ values for various reactions in the Z-range from 22 to 31, using the class K = 4 method of calculation and equation 12 for the level density formula. They then applied these δ values to various other calculated excitation functions. The outcome of these calculations was that better agreement was obtained than with those using Cameron's pairing values. However, it was also established that if they increased the value of r_o from 1.5 fm to 1.7 fm in their equation for the inverse cross section, then the calculations using Cameron's values gave improved agreement. In fact some of the calculations were just as good as those obtained with the special Dostrovsky et al. [5] δ values.

6. The Class K = 5,6 Calculations

These methods of calculations are characterized by a two-step reaction mechanism. The first step initially involves two-body collisions between the projectile and a nucleon, which is then followed by proton-neutron collisions. Monte Carlo techniques are applied to evaluate the probability for prompt knock-on processes, or what may be termed direct processes. The second step is the evaporation of particles from the residual nuclei originating from the intranuclear cascade processes which is evaluated by means of the equilibrium statistical model.

6.1. Deviations of the Calculated Excitation Functions

Nine articles were considered for these methods of calculation and the number of experimentally determined excitation functions per article varied from 3 to 13 (see figure 4). On the average, 6 experimental excitation functions were used for comparitive purposes with proton numbers of the target nuclei ranging from 21 to 91.

The deviations $(\Delta M/M)$, $(\Delta P/P)$,... etc., cannot be correlated directly to the evaporation part of the calculation, since both the prompt knock-on and evaporation processes contribute to the probability of a specific reaction. This also applies to the parameters used in the level density formula in the evaporation part of the calculations.

The deviations $\overline{(\Delta M/M)} \pm \Omega\overline{(\Delta M/M)}$, $\overline{(\Delta P/P)} \pm \Omega\overline{(\Delta P/P)}$, ... etc., are shown in figure 4. No MEAN $\pm$ SD value was calculated for article 24 because of its unusual trend for the deviations. For most of the articles in this work, it was that if $\overline{(\Delta M/M)}$ is positive then $\overline{(\Delta SH/SH)}$ is negative. However, in article 24 $\overline{(\Delta M/M)}$ is positive, but $\overline{(\Delta SH/SH)}$ is also positive.

An average of the MEAN ± SD values gave 15 ± 34 % and 17 ± 46 % for the K = 5 and K = 6 classes respectively. Thus the accuracy of the analytic and Monte Carlo calculations are virtually the same giving an overall average of 16 ± 40 %. The overall agreement between the calculated and experimental values for the maximum cross section M, the position P, the full-width FW and the high-energy slope SH is remarkable over the whole Z-range from 21 to 91.

It is interesting to note that in class K = 5 [articles 23, 21, 22 and 20] the Jackson model [1] was used for the evaporation part of the calculation. This model seems to yield reliable calculated results over the Z-region 68 to 82, i.e. where the emission of charged particles may be neglected.

6.2. Parameters used

The level density formula used in the evaporation part of these calculations is that given by equation 12. The model of Jackson [1], used for calculating neutron emission probabilities only, does not account for individual nuclear properties. For instance, it does not take the differences of

Table V: Values used in the evaporation part of the K = 5,6 calculations; the articles are arranged in increasing order of the Z-range of the target nuclei

Article No. (Class K)	Corrections for the excitation energy U		C [MeV] in eq.	Nuclear temperature T [MeV]
	Eq.	Exponential term	8	
6 (6)	12	δ	20.0	-
11 (6)	12	δ	20.0	-
24 (6)	-	-	-	-
10 (6)	12	δ	10.0	-
23 (5)	Jackson model			2.4
21 (5)	"			1.95
22 (5)	"			1.8
20 (5)	"			1.8
28 (6)	12	δ	-	-

the binding energies of neutrons in the various nuclei into account, but takes one mean value. It also assumes a constant nuclear temperature T (cf. article 20, figure 4 and Table V). As may be seen from figure 4, the agreement between experiment and calculation is exceptional. The suceess of his model is unexpected in view of the stress that was laid on the parameters accounting for individual nuclear properties entering into level density formulae, discussed in the previous sections.

7. The Class K = 7 Calculations

Although relatively few calculations have been performed with the pre-equilibrium model, it has been included for the sake of completion. This class is similar to the K = 5,6 calculations, in that direct processes are also taken into account. The pre-equilibrium model describes an equilibration process between particles and holes and evaluates the fraction of particles emitted. After reaching equilibrium, the fraction of evaporated particles is calculated by the Weisskopf-Ewing formula. The unknowns are the initial number n_i of particles plus holes and the fraction of direct reactions prior to equilibrium - the so-called pre-equilibrium fraction.

Figure 5 shows the deviations for the class K = 7 calculations. With the exception of the calculations in the Z-region between 13 and 23, the deviations are very small indeed. Therefore these calculations may prove to account for the direct processes successfully. However, more comparison with experiment is needed.

Because consistent values for the initial exciton number n_i seem to be forthcoming from the calculations considered here, it is possible to surmise that these calculations will, in future, have one less unknown, viz. n_i. For example, it has been found that for projectiles such as protons and α-particles, $n_i = 3$ and $n_i = 5$ respectively, regardless of the nucleon number of the target nucleus.

8. Conclusions

A summary of methods for calculating excitation functions is given in Table VI. The number of experimental excitation functions used for comparison totals 235. On the average about 6 experimental excitation functions were used per article. About 70 % of the articles have compared their calculations with

Table VI: Data for similar sets of calculation methods

Similar classes	No. of exp. exc. func.	Average No. of exp. exc. func. per article	Z-range of target nuclei	$\overline{MEAN} \pm \overline{SD}$ [%] *
1+2	55	5	13-79	20 ± 37
3+4	105	5	13-82	62 ± 77
				$(37 \pm 60)^+$
5+6	51	6	21-91	16 ± 40
7	24	8	13-83	47 ± 76

* Taking a one sigma confidence limit

\+ See text

various reactions on targets of one element alone. However, the articles used for a class cover a large Z-range. Therefore, the Grand Means $\overline{MEAN} \pm \overline{SD}$ (i.e. the average of the MEAN $\pm$ SD values for similar classes) should give representative overall errors. Excluding the articles 18 and 19 in class K = 3, for reasons mentioned in 5.1, one gets a Grand Mean for the similar classes K = 3,4 of 37 ± 60 %.

According to Table VI the Grand Means for the four sets of similar classes are virtually the same, despite the fact that the various models and methods used for calculations differ considerably as to the sophistication of theory and the number of parameters. The methods K = 5,6 and 1,2 are very time-consuming and require a large computer memory. Therefore, the classes K = 3,4 and 7 seem to be very suitable for fitting many excitation functions. But in all cases it is almost impossible

to make a reliable estimate for the input parameters to predict excitation functions over a wide range of target nuclei, reaction-types and excitation energies.

9. References

1. J.D. Jackson, Can. J. Phys. 34 (1956) 767

2. J. Lange and H. Münzel, KFK 767 (1968)

3. S. Fukushima, S. Kume and H. Okamura, Nucl. Phys. 69 (1965) 273

4. A.G.W. Cameron, Can. J. Phys. 36 (1958) 1040

5. I. Dostrovsky, Z. Fraenkel and G. Friedlander, Phys. Rev. 116 (1959) 683

10. Appendix A

Listed below are the references of the 30 articles used in this survey.

1. H. Kurz, Dissertation Universität Bonn (1969)
2. F.H. Ruddy, B.D. Pate and E.W. Vogt, Nucl. Phys. A127 (1969)323
3. R.A. Esterlund and B.D. Pate, Nucl. Phys. 69 (1965) 401
4. S. Fukushima, S. Hayashi, S. Kume, H. Okamura, K. Otozai, K. Sakamoto and Y. Yoshizawa, Nucl. Phys. 41 (1963) 275
5. S. Fukushima, S. Kume, H. Okamura, K. Otozai, K. Sakamoto and Y. Yoshizawa, Nucl. Phys. 69 (1965) 273
6. T. McGee, C.L. Rao, G.B. Saha and L. Yaffe, Nucl. Phys. A150 (1970) 11
7. D. Sperber, Phys. Rev. 178 (1969) 1688
8. D.G. Sarantites and B.D. Pate, Nucl. Phys. A93 (1967) 545
9. D.G. Sarantites, Nucl. Phys. A93 (1967) 567
10. J.J. Hogan, J. Inorg. Nucl. Chem. 33 (1971) 3627
11. G.B. Saha, N.T. Porile and L. Yaffe , Phys. Rev. 144 (1966) 962
12. I. Dostrovsky, Z. Fraenkel and G. Friedlander, Phys. Rev. 116 (1959) 683
13. N.T. Porile, S. Tamara, H. Amano, M. Furukawa, S.Iwata and M. Yagi, Nucl. Phys. 43 (1963) 500
14. J. Sau, A. Demeyer and R. Chéry, Nucl. Phys. A121 (1968) 131
15. C. Birattari, E. Gadioli, A.M. Grassi-Strini, G. Strini, G. Tagliaferri and L. Zetta, Nucl. Phys. A166 (1971) 605
16. F.M. Lanzafame and M. Blann, Nucl. Phys. A142 (1970) 545
17. M. Blann and F.M. Lanzafame, Nucl. Phys. A142 (1970) 559
18. Yu-Wen Yu and M. Blann, Phys. Rev. 170 (1968) 1131

19. W.W. Bowman and M. Blann, Nucl. Phys. A131 (1969) 513

20. J.D. Jackson, Can. J. Phys. 34 (1956) 767

21. C.L. Rao and L. Yaffe, Can. J. Chem. 41 (1963) 2516

22. G.R. Grant and L. Yaffe, Can. J. Chem. 41 (1963) 2533

23. G.V.S. Rayudu and L. Yaffe, Can. J. Chem. 41 (1963) 2544

24. V.P. Narang and L. Yaffe, Can. J. Chem. 46 (1968) 3171

25. D. Vinciguerra, K. Kotajima and R.E. van de Vijver, Nucl. Phys. 77 (1966) 337

26. N.E. Scott, J.W. Cobble and P.J. Daly, Nucl. Phys. A119 (1968) 131

27. M. Furukawa, Nucl. Phys. A90 (1967) 253

28. R.L. Hahn, K.S. Toth and M.F. Roche, Nucl. Phys. A185 (1972)252

29. M. Furukawa, Nucl. Phys. 77 (1966) 565

30. A. Demeyer, N. Chevarier, A. Chevarier and Tran Minh Duc, J. Phys. (Paris) 32 (1971) 583

Deviations of Calculated Excitation Functions for Classes K=1, K=2

Class K	1	2	1	1	1	1	2	1	2	1
Article No.	19	8	2	3	30	7	9	14	1	16
No. Exp. Exc. Func.	8	4	5	9	4	2	3	4	12	4
Z of Targets	13-23	30	30	30-67	37	47	47	67	79	79
Energy Range	7-120	8-34	5-40	4-32	10-60	10-40	10-36	15-55	17-100	19-100

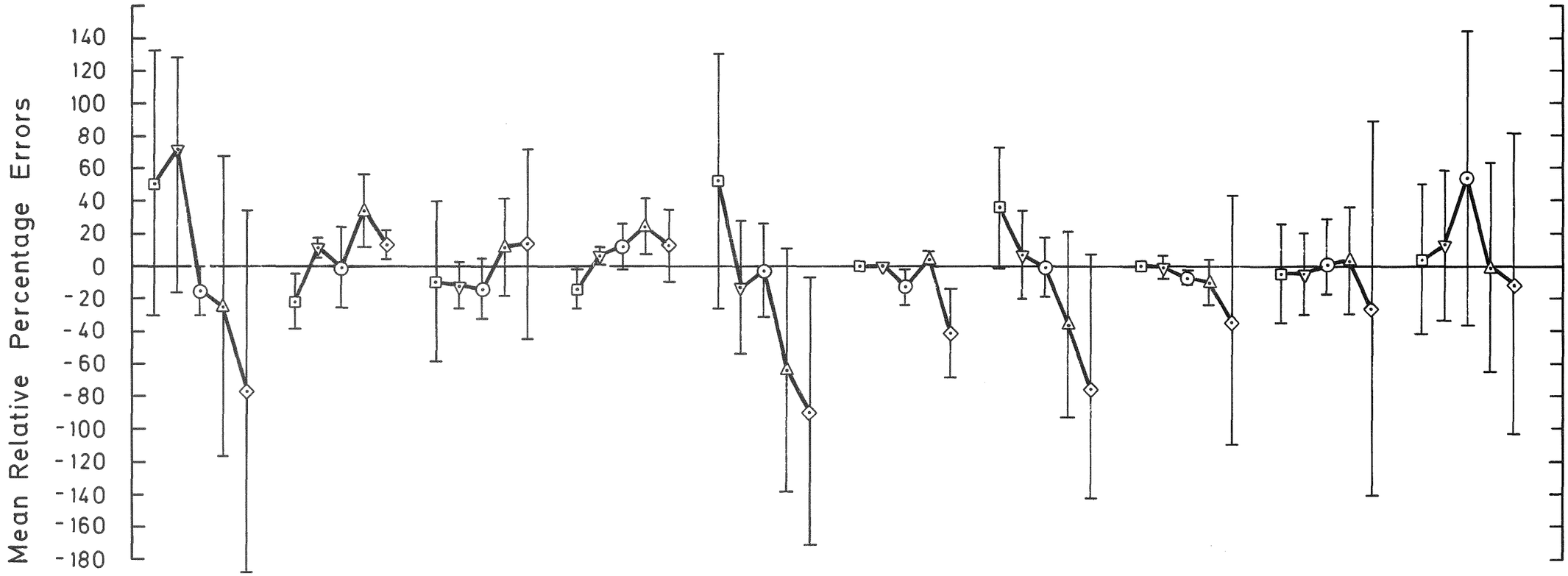

MEAN ± SD	(48 ± 71)	(16 ± 16)	(12 ± 34)	(14 ± 14)	(44 ± 61)	(12 ± 9)	(31 ± 41)	(10 ± 25)	(8 ± 46)	(17 ± 68)

Figure 2. ⊡ $\overline{(\Delta M/M)}$, ▽ $\overline{(\Delta P/P)}$, ⊙ $\overline{(\Delta FW/FW)}$, △ $\overline{(\Delta SL/SL)}$, ◇ $\overline{(\Delta SH/SH)}$: Error Bars = ± Ω $\overline{(\Delta M/M)}$,....

Deviations of Calculated Excitation Functions for Classes K=3, K=4

Class K	3	4	4	4	4	3	3	3	3	3	3	3	4
Article No.	19	6	12	13	11	18	4	5	29	27	16	25	26
No.Exp.Exc.Func.	7	9	40	12	8	6	6	3	2	2	4	3	3
Z of Targets	13-23	21-30	22-31	32	39	40	47	47	57	58	79	79	82
Energy Range	7-120	10-85	0-50	13-56	5-85	25-80	10-40	10-40	11-40	0-14	19-100	23-52	10-40

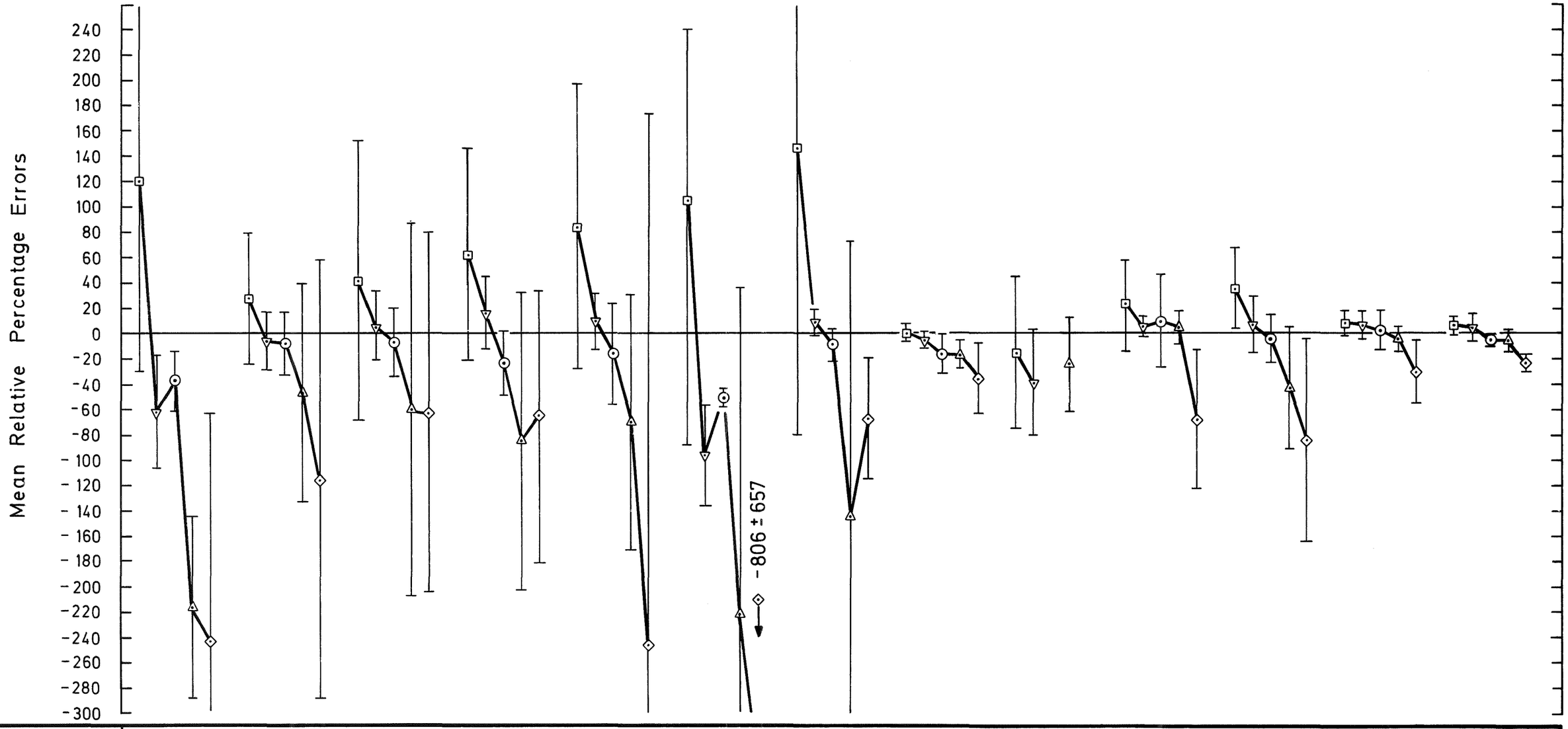

MEAN ± SD	(136±94)	(41±72)	(35±91)	(52±71)	(85±139)	(256±231)	(75±103)	(15±28)	(—)	(22±30)	(35±40)	(11±14)	(9±8)

Figure 3. $\boxdot\,\overline{(\Delta M/M)}$, $\triangledown\,\overline{(\Delta P/P)}$, $\odot\,\overline{(\Delta FW/FW)}$, $\triangle\,\overline{(\Delta SL/SL)}$, $\diamond\,\overline{(\Delta SH/SH)}$, : Error Bars = $\pm\,\Omega\,\overline{(\Delta M/M)}$,....

Deviations of Calculated Excitation Functions for Classes K = 5, K = 6

Class K	6	6	6	6	5	5	5	5	6
Article No.	6	11	24	10	23	21	22	20	28
No.Exp.Exc.Func.	9	8	4	4	3	4	3	13	3
Z of Targets	21-30	39	53	59	68	73	77	82	90-91
Energy Range	10-85	5-85	0-80	0-90	6-87	8-84	9-87	8-80	30-80

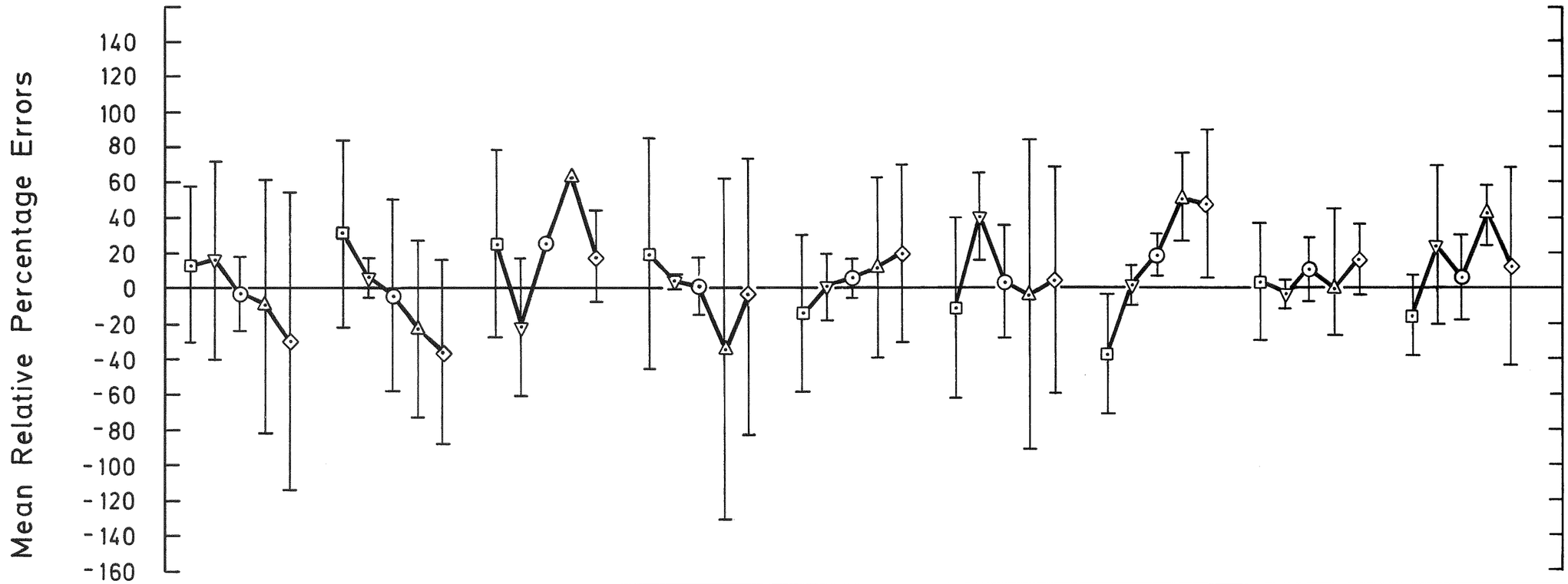

MEAN ± SD	(14±55)	(20±44)	(—)	(13±52)	(10±35)	(13±52)	(31±25)	(6 ±25)	(20±33)

Figure 4. ⊡ $\overline{(\Delta M/M)}$, ▽ $\overline{(\Delta P/P)}$, ⊙ $\overline{(\Delta FW/FW)}$, ▽ $\overline{(\Delta SL/SL)}$, ◇ $\overline{(\Delta SH/SH)}$: Error Bars = ± Ω $\overline{(\Delta M/M)}$,....

Deviations for Class K = 7

Class K	7	7	7
Article No.	19	17	15
No.Exp.Exc.Func.	7	11	6
Z of Targets	13-23	23-79	69-83
Energy Range	7-120	20-45	19-100

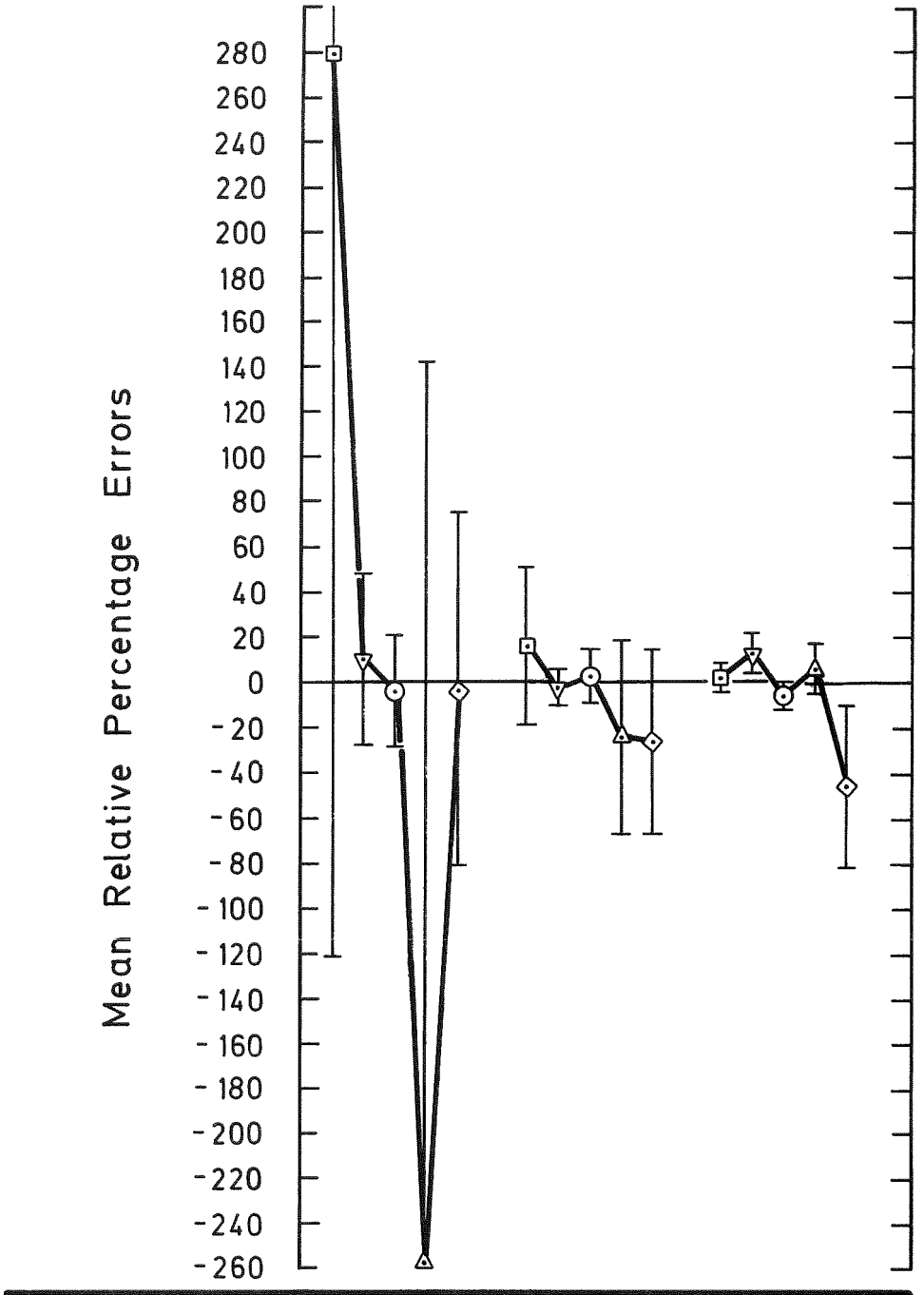

MEAN ± SD	(111±188)	(14±28)	(15±13)

Figure 5: Symbols as for Figure 4.